Wind and Structures, Vol. 3, No. 1 (2000) 59-67
DOI: http://dx.doi.org/10.12989/was.2000.3.1.059

Wind-induced fatigue design of a cruciform shaped mast

P. A. Mendis†

Department of Civil and Environmental Engineering, The University of Melbourne, Victoria 3052, Australia

B. Dean‡

Connell Wagner Ltd., Victoria, Australia

Abstract: The cruciform shaped mast over 47 storey, Telecom Corporate Building in Melbourne, Australia rises to a height of approximately 25 m above the roof level. As the members are subjected to very high fluctuating loads under wind, the design was mainly governed by wind-induced fatigue. A detailed fatigue analysis was carried out according to the requirements of the Australian Steel Structures Code, AS4100. The wind-induced fatigue analysis procedure is described in the paper. The fatigue design of this mast is used as an example to illustrate some potential problems of relevant specifications in AS4100 and to outline some of the more important parameters in the fatigue analysis.

Key words: wind-induced fatigue; masts; steel; hollow sections; codes of practice.

1. Introduction

The Telecom corporate building is a 47 storey building, approximately 196m above ground level and is situated in Melbourne, Australia. The cruciform shaped mast over the Telecom building rises to a height of approximately 25 m above the roof level. The structural design of the building and the mast was carried out by Connell Wagner (Vic) Ltd. The architectural and construction requirements led to the selection of a relatively light weight cruciform shaped structure (Fig. 1). It consists of four 305×305×12 square hollow sections welded together (Fig. 2). The mast was connected to the main tower at 2 levels as shown in Fig. 1.

The dynamic analysis gave a fundamental natural frequency of 0.9 Hz for the mast. This frequency was calculated considering the isolated mast, i.e., ignoring the building. To increase the cross-wind damping of the structure a hanging chain damper was provided at the top. The chain damper was 2.83 m long and designed to provide 2% damping. It was hung from the top section of the central tube. The mass/length of the chain was 32.5 kg/m. Also 4.5 m length of the mid section of the mast was filled with cementitious grout to increase the damping and to improve the stability of the top connection to the building. The grout was produced from a 6 : 1 (cement:sand) mix. Extra damping is provided by the additional mass and the microcracks formed within the grout.

The mast was designed for a design life of 100 years. During that time, the members are subjected

† Senior Lecturer
‡ Principal

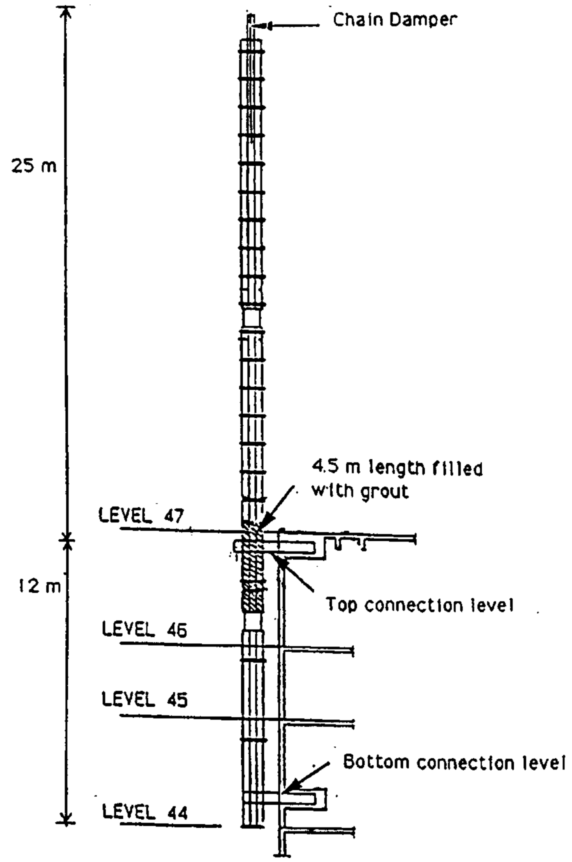

Fig. 1 Mast elevation

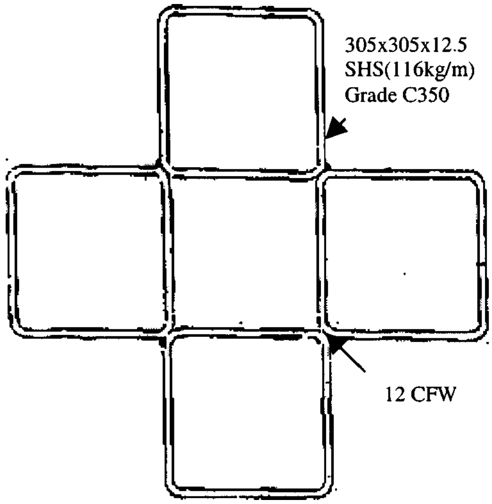

Fig. 2 Mast cross-section

to a very large number of cycles of fluctuating wind loads. Therefore the design was mainly governed by wind-induced fatigue. A detailed fatigue analysis was carried out by the authors according to the requirements of the Australian Steel Structures Code, AS4100 (1990). As mentioned earlier the dynamic analysis was conducted ignoring the effects of the building vibration. However a special study was conducted later to investigate the effects of the interaction between the mast and the building. These effects were found to be insignificant. Therefore only the isolated mast was considered in the fatigue analysis.

The main purpose of this paper is to present a case study to illustrate the wind-induced fatigue design procedure and to demonstrate the application of the steel structures code. There are still a number of unidentified potential problems in fatigue design specifications given in Codes of Practice. Some of them are identified in this paper.

2. Wind-induced fatigue analysis

2.1. Calculation of number of cycles

The probability of the wind speed being in a given band may be derived from available hourly mean wind data. The probabilities for this fatigue analysis were obtained by fitting a weibull distribution for wind data from the Essendon Airport in Melbourne (Melbourne 1990).

For this particular case, the probability of exceeding a given velocity, $P(>V)$, was given by the following expression.

$$P(>V) = e^{-(0.15V)^{1.42}} \tag{1}$$

Where V is the gust wind speed at 10 m height, Terrain category 2, in m/sec (AS1170 Part II-1989). This equation was derived for the most critical direction (i.e., west).

The probabilities given by the above equation were converted to number of stress cycles in each wind speed band within the design life of the structure by a direct transformation as given in Eq. (2).

$$\text{No. of cycles} = \text{Prob.} \times n_a \times 365 \times 24 \times 3600 \times N \tag{2}$$

n_a – Natural frequency (Hz.)
N – Design life (taken as 100 yrs.)

The wind-induced random fatigue loading is not considered in the simple equation given above.

2.2. Calculation of stress ranges for each wind speed band

The wind forces acting on wind sensitive structures depend on wind speed, terrain, dynamic response of the structure and cross-wind effects. The wind-induced fatigue occurs as a result of the along-wind and cross-wind response of the structure. The cross-wind response is mainly caused by vortex shedding and is a major problem for long slender solid towers or elements on towers.

The sinusoidal lock-in and random excitation models (Saunders and Melbourne 1975, Kwok and Melbourne 1981) were used for the preliminary cross-wind design of this structure. The along-wind effects were evaluated by the gust factor method described in AS1170.2 (1989) and assuming a terrain category of 2. The gust factor was found to be approximately 2.03. As this shape is not covered in the code an estimated drag coefficient was used in the preliminary analysis. The average value (equal to 1.75) for sharp-edged (equal to 2.2) and smooth-edged square shapes (equal to 1.3) given in the code was selected as the drag coefficient.

2.3. Wind tunnel testing

Because of the unusual shape, the only reliable means to predict the dynamic response of this wind sensitive structure was to test in a wind tunnel. The wind tunnel testing was carried out to check the possibility of "galloping instability" and to obtain better estimates of cross-wind and along-wind loading.

The wind tunnel tests were carried out in the 450 kW boundary layer wind tunnel at the Department of Mechanical Engineering, Monash University. An aeroelastic model of the mast was built to a length scale of 1/57.5 and a density ratio of 1.0. The wind moment envelope derived from wind tunnel results for different wind directions is shown in Fig. 3. The wind tunnel tests gave both along-wind and cross-wind response effects. As seen from the graphs the wind design was governed by the along-wind response rather than the cross-wind response. The maximum along-wind moment occurred at $\beta = 0^{\circ}$ (Fig. 3). At that location, the cross-wind moment was negligible. Also it was shown that there was no evidence of galloping instability at 1% damping.

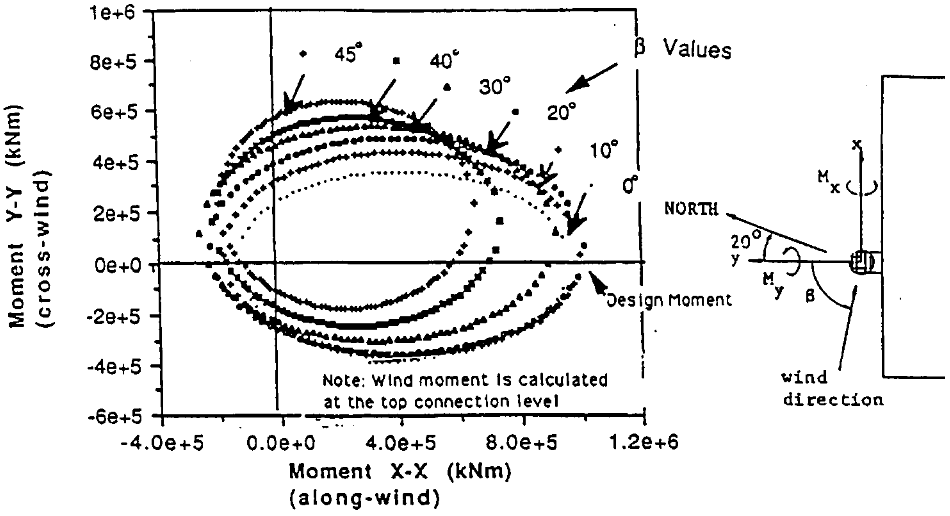

Fig. 3 Moment envelope

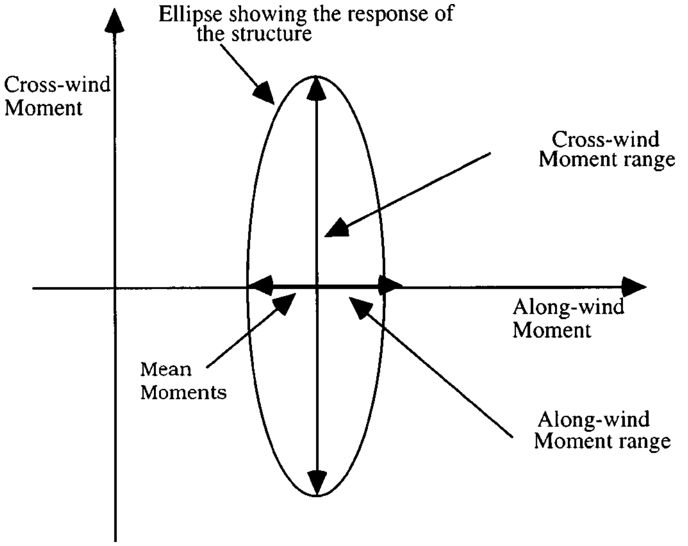

Fig. 4 The response of the structure for a particular wind direction

As mentioned earlier, a drag coefficient of 1.75 was used to calculate the along wind moments in the preliminary analysis. As seen from the wind envelope the maximum along-wind moment is approximately 1010 kNm. This moment gave an equivalent drag coefficient of 1.3. As expected the wind tunnel results in the cross-wind direction were significantly lower than (up to 50%) the estimated values using the sinosoidal lock-in and random excitation models.

An ellipse representing the response of the structure for a particular wind direction is shown in Fig. 4. The along-wind and cross-wind moment ranges were extracted from these ellipses. These moment ranges were converted to stress ranges by applying an appropriate section property relationship. A damping ratio of 2% was used in the final design. This figure was verified during the fabrication stage. The extra damping effect from the hanging chain damper was ignored in the analysis.

3. Fatigue analysis

A detailed fatigue analysis was carried out according to the requirements of the Australian Steel Structures Code, AS4100. The fatigue design rules in AS4100 are derived from the ECCS (1985) recommendations. Detail category (f_{rn}) is the designation given to a particular detail to indicate which of the S (Stress range)-N (Number of stress cycles) curves is to be used in the fatigue assessment. The detail category takes into consideration the local stress concentrations at the detail, the size and shape of the maximum acceptable discontinuity, the loading condition, metallurgical effects, residual stresses, the welding process and any post weld improvement. The detail category number (f_{rn}) is defined by the fatigue strength at 2×10^6 cycles on the S-N curve. S-N curves for normal stress are given in Fig. 5. In this figure, the constant stress range fatigue limit (f_3) is the highest constant stress range for each detail category at which fatigue cracks are not expected to propagate. The cut-off limit (f_5) is the highest variable stress range for each detail category which does not require consideration when carrying out a fatigue analysis.

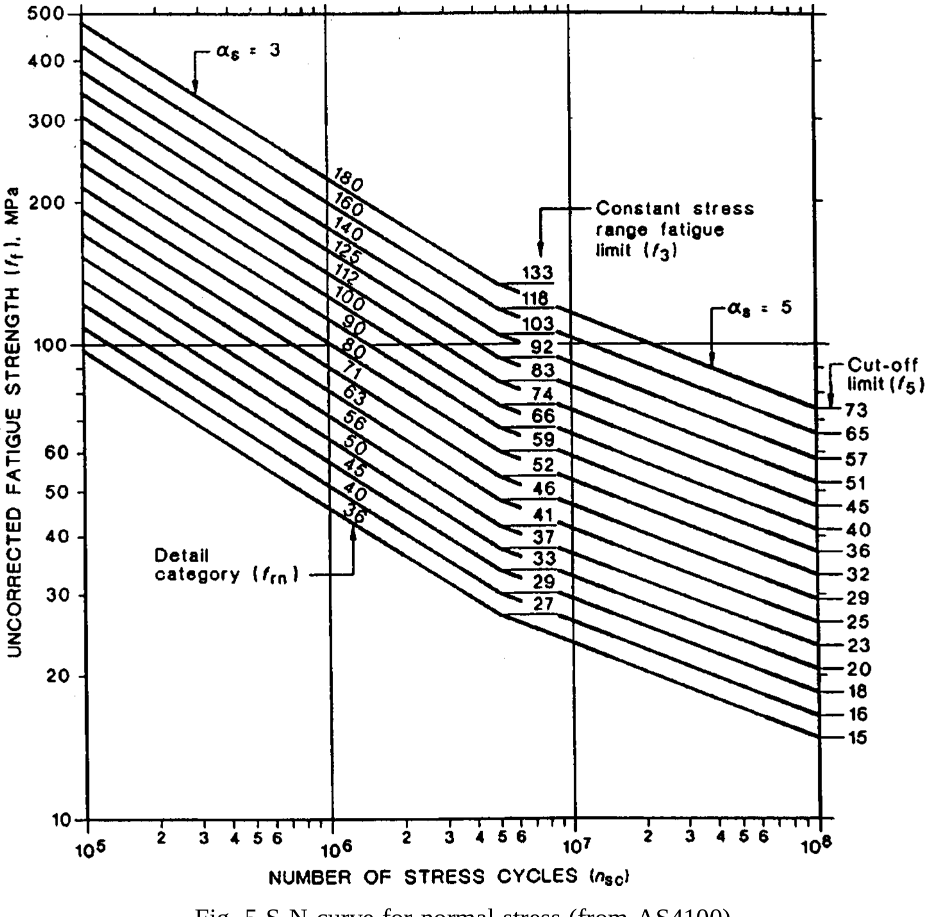

Fig. 5 S-N curve for normal stress (from AS4100)

The first step in the fatigue design was to select the detail category and the stress due to maximum wind speed. If the stress due to maximum wind speed was less than the constant stress range fatigue limit or the cut-off limit the fatigue assessment was not required. Otherwise the Miner's rule given in Eq. (3) was used to calculate the cumulative damage.

$$\frac{\sum_i n_i (f_i^*)^{\alpha_s}}{n_r (\phi f_f)^{\alpha_s}} \leq 1.0 \tag{3}$$

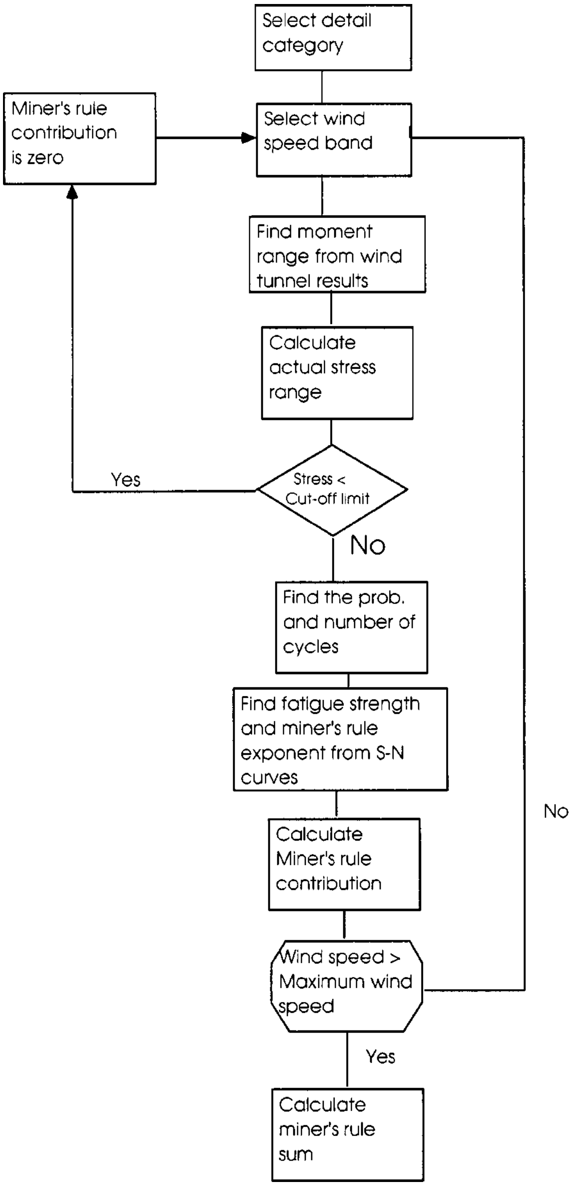

Fig. 6 Flow chart for cumulative damage calculations

Table 1 Fatigue detail categories

Component	Category
1. Main Section (4 SHS)	
(i) With welded attachments	71
(ii) Without welded attachments	140
2. Effect of longitudinal fillet weld on SHS	90
3. Top connection (stresses from finite-element analysis)	71
4. Bottom connection	125
5. Splice location	
(i) Bolts (TF)	Not reqd.
(ii) Plates	80
(iii) Weld	80
(iv) SHS at splice location	50

where n_i is the number of cycles of nominal loading event i, producing a design stress range of f_i^*. α_s is the inverse of the slope of the S-N curve (see Fig. 5). n_r is the reference number of stress cycles (2×10^6). ϕ is a capacity factor. f_f is the fatigue strength found from Fig. 5. Although the allowable total sum in Eq. (3) is 1.0, it was decided to adopt a conservative approach by limiting the sum to not more than about 0.75. This limit was considered to be appropriate due to some assumptions made in the analysis such as ignoring the effects of the interaction between the mast and the building and the effects of random wind-induced along wind loading.

A computer program was written to perform these operations. The flow chart is given in Fig. 6. The fatigue detail categories used for different components are shown in Table 1.

4. Conclusions

1. Wind-induced fatigue governed the design of this cruciform shaped mast. More wind tunnel tests on cruciform shaped sections are required to derive generalised coefficients for the wind code.
2. As mentioned before detailed fatigue calculations are required when the stresses are higher than either the constant stress range limit or the cut-off limit. Use of Miner's rule for cumulative damage calculations is a tedious process. However a computer program or a spread-sheet would facilitate this process.
3. It is important to identify the reduction of fatigue capacity by welded attachments. The graph of Miner's rule sum for longitudinal stresses at main cross-section (4 SHS) with and without welded attachments vs distance from top connection level is shown in Fig. 7. As seen welded attachments could not be used at top connection level.
4. The high stress-low cycle fatigue is not covered in AS4100. However the code specifies an upper limit of $1.5F_y$ for the stress range. For this analysis different S-N curves given in AS4100 were extrapolated up to a maximum limit of F_y. The Miner's rule sum is very sensitive to this value. There was a significant reduction in Miner's rule sum when the upper limit was increased to $1.5F_y$. The effect of this change is illustrated in Fig. 7.
5. According to AS4100 a capacity factor (ϕ) of less than or equal to 0.7 should be used for non-redundant paths. The graph of Miner's rule sum vs. capacity factor for longitudinal stresses at

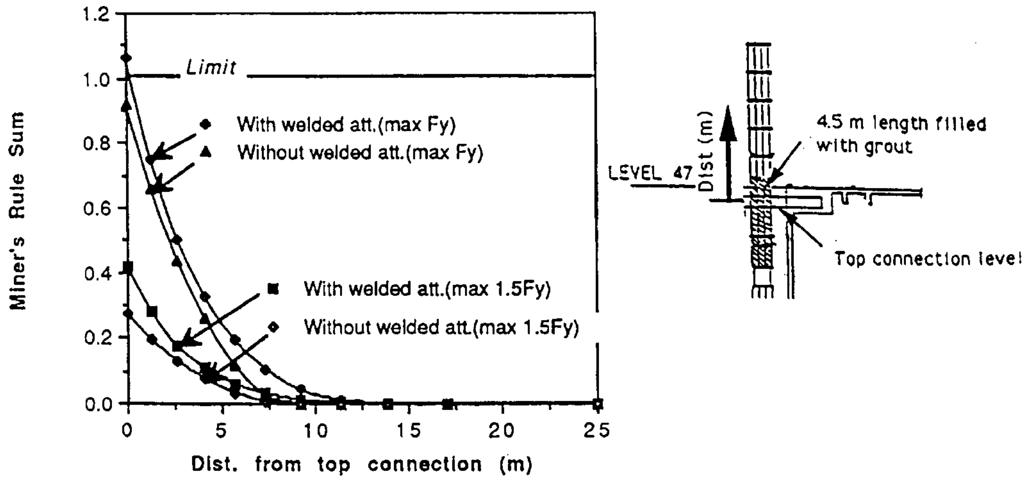

Fig. 7 Graph of Miner's rule sum versus distance from top connection for mast cross section

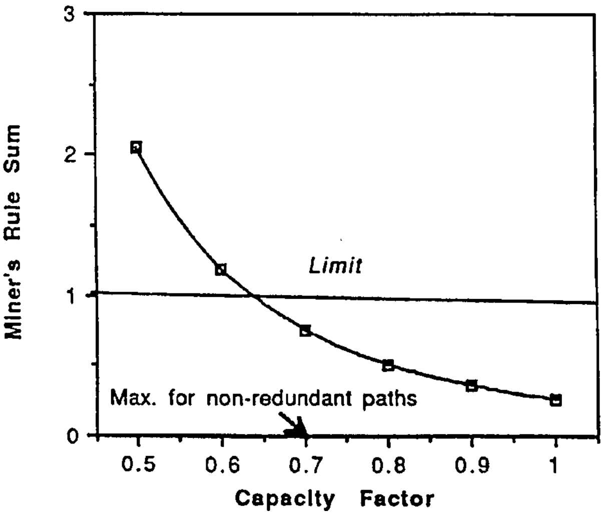

Fig. 8 Graph of Miner's rule sum versus capacity factor for mast cross section

main cross-section (4 SHS) is given in Fig. 8. This graph shows the sensitivity of the capacity factor. The final fatigue assessment is dependent on the selection of the capacity factor. Therefore it is very important to select the appropriate capacity factor.

6. A very accurate fatigue analysis is required for this type of structure. As seen from Table 1, detail categories given in AS4100 covered the different locations adequately for this mast.

References

European Convention for Constructional Steelwork. (1985), "Recommendations for the fatigue design of structures", ECCS-TC-6.

Kwok, K.C.S. and Melbourne, W.H. (1981), "Wind-induced lock-in excitation of tall structures", *Journal of the Structural Division, ASCE*, **107**(1), 57-72.
Melbourne, W.H., "Wind data for Melbourne", private communication, 1990.
Saunders, J.W. and Melbourne, W.H. (1975), "Tall rectangular building response to cross-wind excitation", *Proceedings of the 4th International Conference on Wind Effects on Buildings & Structures*, University Press, 369-379.
Standards Association of Australia, "Steel structures", AS 4100, 1990.
Standards Association of Australia, "SAA loading code Part II: wind loads", AS 1170.2, 1989.

(*Communicated by Chang-Koon Choi*)